XVIII IMEKO WORLD CONGRESS
Metrology for a Sustainable Development
September, 17 – 22, 2006, Rio de Janeiro, Brazil

FAULT ACCOMMODATION OF MASS AIR FLOW SENSORS IN DIESEL AUTOMOTIVE ENGINES

Giovanni Betta [1], *Domenico Capriglione* [1], *Antonio Pietrosanto* [2]

[1] DAEIMI, University of Cassino, Via G. Di Biasio 43, 03043 Cassino (FR), ITALY, E_mail: {betta, capriglione@unicas.it }
[2] DIIIE, University of Salerno, Via P. Don Melillo 1, 84084 Fisciano (SA), ITALY, E_mail: apietrosanto@unisa.it

Abstract: This paper deals with the design and the application of Artificial Neural Networks to the fault accommodation of the mass air flow meter in diesel engines. Several architectures are proposed and tested. In order to verify their real applicability to the automotive context, making use of suitable graphical tools and computational load indexes, their performance was compared in terms of accuracy and resource requirements.

Keywords: Instrument fault accommodation, Artificial Neural Networks (ANNs), Mass air flow meter.

1. INTRODUCTION

Modern transportation vehicles are equipped with a lot of electronic devices devoted to grant passenger safety and comfort (Anti-lock braking system, Anti-spin regulation, Electronic stability program, Airbag, air conditioning, and so on), as well as to control fuel injection, ignition and the pollution emissions of the engines. The correct operating of such systems depends on the accuracy of the collected measurements and on both the reliability and the status (faulty-free or faulty) of the corresponding sensors [1], [2]. Usually engine operating is strongly based on the measurements performed by the sensors providing information about power and torque driver needs, engine speed and intake manifold air quantities. A suitable electronic control unit processes these quantities defining the ignition times and their durations with the aim of accomplishing the more and more severe legislation limits on the pollution emissions and of optimizing the engine working. Indeed, the requirements for lower limits of exhaust gasses are today only achievable with electronic engine management [3].

The challenge in engine fueling control is the coordination of air and fuel entrainment into the engine cylinders. Modern direct-injected diesels include well-developed combustion systems that have electronically controlled injection systems and robust turbochargers. In particular, the measurement of the mass air flow in the intake manifold plays a critical role in the process of estimating fuel to be injected [4].

On the other hand, mass air flow sensors are subjected to aging phenomena due to the amassing of combustion residuals on the sensing element. These events often bring to measurement errors greater than 20 % that compromise the correct working of the engine in terms of exhaust gasses emissions and vehicle performance. Unfortunately, the former symptom cannot be detected by the user while the latter is very ambiguous.

As a consequence, a great effort has been driven to design and set-up instrument fault detection and isolation schemes (IFDI), able to identify the mass air flow sensor faults [5-9]. However, once the fault has been detected a further problem remains: due to the high time to repair and often to the scarce availability of substitute, faulty vehicles keep on circulating with negative consequence on safety and pollution. A further improvement to the safety granted in automotive systems by IFDI schemes could be provided by implementing in measurement systems also the capability of sensor fault accommodation, thus avoiding even the malfunctioning or in some cases the stop of the vehicle. Once the mass air flow sensor fault has been detected, an accommodation module should predict the quantity in substitution of the faulty sensor on the basis of the other sensor outputs, thus allowing the ECU control software to work properly as consequently make the engine and vehicle. This feature is rarely implemented on modern vehicles. Whenever it happens, due to the difficulty in modeling the engine physics, the feature implemented is closer to a recovery procedure rather than an accommodation one.

The authors experimented the use of artificial intelligence techniques in the realization of IFDIA schemes for automotive systems [10-12]. The good performance in terms of promptness, sensitivity and accuracy obtained in the diagnosis and the accommodation of faults in the sensors of a FIAT 1,242 litres Spark Ignition Engine suggest and even encourage the use of these techniques also for diesel engines. Focusing the attention on the accommodation section, in this paper, several ANN-based architectures are proposed to overcome the faults that could occur on the mass air flow sensor employed in modern diesel turbocharged engines. They will be developed for two of the most widespread diesel technologies, common rail and injection pump. A suitable comparisons among the proposed architectures is reported in detail.

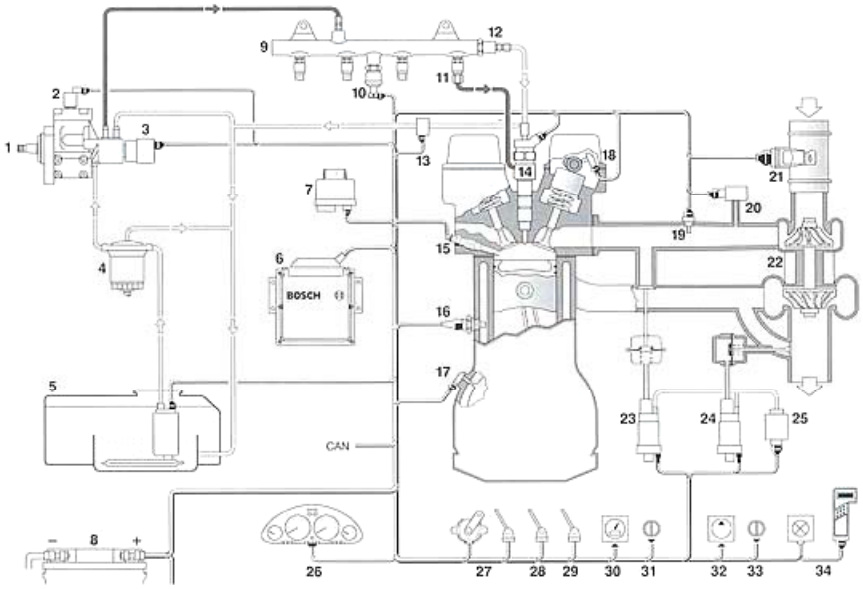

1:High-pressure pump
2:Element switchoff valve
3:Pressure-control valve
4:Fuel filter
5:Fuel container
6:ECU
7:Glow control unit
8:Battery
9:High-pressure accumulator
10:Rail sensor
11:Flow limiter
12:Pressure limiter
13:Fuel temperature sensor
14:Injector
15:Glow element
16:Coolant temperature sensor
17:Crankshaft speed sensor
18:Camshaft speed sensor
19:Intake air temperature sensor
20:Boost-pressure sensor
21:Air mass sensor
22:Turbocharger
23:Exhaust-gas recirculation positioner
24:Charge.pressure actuator
25:Vaccum pump
26:Speedometer
27:Gas pedal
28:Brake contacts
29:Clutch switch
30:Vehicle speed sensor
31:Vehicle speed controller
32:Air-conditioner compressor
33:Control panel for Air-conditioner compressor
34:Connector for diagnostic device

Fig. 1. Sketch of common rail system (in bold the main components used for the engine management)

2. THE SYSTEMS UNDER ANALYSIS

As above mentioned, modern diesel turbocharged engines operate on the basis of the measurements performed by a wide set of sensors. As an example in Fig.1 a sketch of a *common rail* system is reported, but similar schemes and considerations could be made for *injection pump* engines. The main difference, in fact, between these two systems is the high-pressure accumulator (rail) that is absent in injection pump systems. In both cases they are "drive by wire" systems in which the electronic control unit (ECU) decides the fuel quantity to be injected, the time and the duration of the injection on the basis of the following quantities:

- accelerator position;
- crankshaft speed;
- intake mass air flow;
- battery voltage;
- air temperature;
- coolant liquid temperature;
- fuel pressure;
- boost pressure.

Practically, only the first three quantities assure the basic information for the fuel control strategy whilst others are used to give further corrections to the time and duration of the fuel injection. As matter of fact, the Accelerator Position (*A*), the Crankshaft Speed (*S*), the intake mass air flow (*M*) and boost-pressure (*P*) are correlated quantities since the most recent fueling control systems operate in a reactive mode: the driver input directly moves the accelerator and the ECU calculates the time and the duration of the fuel to be injected, on the basis of the current values of the engine speed and the mass air flow. Result of this action is a new engine operating state and thus, new values of *S*, *M* and *P*. The analytical relationships representing both physical phenomena and control strategies would allow to design analytical redundancy-based schemes to the fault accommodation of the mass air flow sensor.

Unfortunately, these analytical links are not easy to be identified and, when available, they usually model the process only in steady-state conditions [4], thus not allowing robust residuals to be generated. Aim of the authors' work was the realization of a robust scheme for the mass air flow meter fault accommodation in any vehicle and engine working conditions. As explained in the following sections the goal has been reached thanks to the extrapolating and regression properties of ANN-based architectures [10-12].

3. THE PROPOSED SOLUTION

The solution proposed by the authors is based on three fundamental points: i) the dynamic behavior of the system can be better modeled by suitably designed and trained ANNs, than analytical relationships. ii) typical ANN performance indexes like Mean Absolute Error (MAE) or the Mean Square Error (MSE) are not suitable (too much synthetic) to evaluate the performance of ANNs whose task is reproducing time after time the value assumed by a physical quantity. As a consequence, other performance indexes must be found and experienced. iii) the dependence of the mass air flow from the other three measured quantities (*A*, *S* and *P*) is so strong that even combinations of only two of them allow the accommodation to be well performed.

On the basis of these premises, first task of the authors has been designing, training and testing an ANN based module for the accommodation of the air mass flow sensor. In real applications like this, where choices are driven by real-time implementation needs, the maximum effort had to be made to achieve a right trade-off between regression accuracy and execution time. To this aim, several combinations of ANN design parameters such as the type of different input quantities, the number of samples for each input quantity, and ANN internal parameters (hidden nodes, hidden layers, activation functions) were considered. Fig. 2 shows the

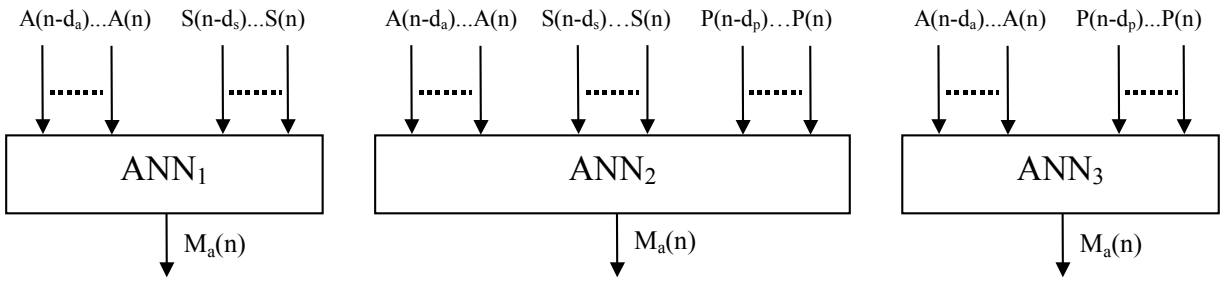

Fig. 2. The ANN architectures for the accommodation of mass air flow sensor

possible ANN-based architectures to the fault accommodation of the mass air flow sensor. As for ANN_1, the accommodated value (M_a) at instant *n* is obtained starting from the values of *A* and *S* at the same instant *n*, and from their values at previous instants. The number of past samples of *A* and *S* to be considered (d_a and d_s, respectively) depends on the time dynamics of the involved quantities and on the reconstruction accuracy required. In addition, it should be taken into account that, the higher number of samples, the greater the computational burden. Similar considerations can be made for ANN_2 and ANN_3 that differ from ANN_1 only for the number and type of different input quantities (Fig. 2). As you can see, the accelerator position is always present as input quantity for the following main reasons: i) *A* is the main information used by the ECU software; ii) *M* strictly depends on *A*; iii) *A* can be considered as an high-reliable quantity because, generally, provided by a double track potentiometer that implements intrinsically a physical redundancy.

All the three ANNs adopt a Multi-Layer Perceptron (MLP) architecture with one hidden layer and one output node. The activation function implemented in the hidden and output layers are hyperbolic tangent sigmoid and natural logarithm sigmoid transfer functions, respectively. Other parameters were instead changed during the tests: the number of hidden nodes (5, 10, 15, 20 and 25) and the number of inputs (spacing from 2 up to 12 for ANN_1 and ANN_3, and spacing from 3 up to 18 for ANN_2, depending on the delay chosen for the input quantities).

Matlab™ was used to train and test the ANNs. The learning sets were made of about 100000 actual samples spaced of $T_S = 500\ ms$ and acquired in many fault-free engine working states and environmental conditions for both common rail and injection pump systems. A Levenberg-Marquardt back-propagation algorithm running on training set was used and a validation set based early stopping was adopted to assure the best performance in terms of accuracy and generalization capability. ANNs performance was evaluated by considering test sets different from the ones used to train the ANNs. As previously said, in order to select the ANN architecture granting the best performance, suitable indexes were searched and adopted.

4. ANN PERFORMANCE COMPARISON

In this section some suitable methods useful to compare the performance of artificial neural networks are described. Rather than using synthetic indexes such as the MAE or the MSE that provides only information about the overall performance of an ANN, some graphical instruments useful to provide both synthetic and detailed indications about performance are considered to better compare the proposed architectures and highlight their features. To this aims the *Regression Error Characteristics (REC) curves* [13] and a novel tool proposed by the authors, the *Sliding Occurrence Error curves* were considered. The performance comparison was then completed by the analysis of the *computational burden* needed in run-time by each ANN architecture.

4.1. Regression Error Characteristics curves

Regression Error Characteristics (REC) curves plot, for each point (x, y), the *relative occurrences* of regression function outputs (on the *y*-axis) that are within a given *error range* (tolerance) (on the *x*-axis). The resulting curve estimates the cumulative distribution function (CDF) of the error [13]. The *error* is defined as the difference between the regression function output (ANN output in the our case), M_a and the actual value, y. It could be the squared deviation $(y - M_a)^2$ or the absolute deviation $|y - M_a|$ depending on the error metric employed. Both relative and percentage deviations can be used. If we impose a zero tolerance, only those points that the regression function fits exactly would be considered as "accurate". If we choose a tolerance that exceeds the maximum error observed on all of the data, then all points will be considered as "accurate".

Main properties of REC curves are:

i) easy visual comparison among different regression functions (ANNs);
ii) the area over the curve (AOC) is a biased estimate of the expected mean error and provides a measure of the mean accuracy; the closer the curve to *y*-axis the better performance are expected for the regression function;
iii) an effective strategy is given to see when regression ANN performance are alike and when they are quite different; REC curves provide a much more compelling presentation of regression results than alternatives such as tables of mean squared errors;
iv) the information represented in REC curves can be used to guide the modelling process based on the goals of the modeller.

As an example, Fig.3 shows REC curves for six different regression functions. As you can see, the regression function *2* offers the worst performance in terms of absolute deviation, whilst the regression functions *3* and *4* show a comparable behaviour.

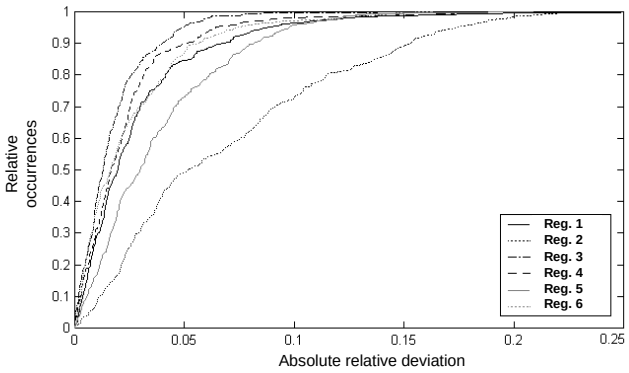

Fig. 3. REC curves for different regression functions.

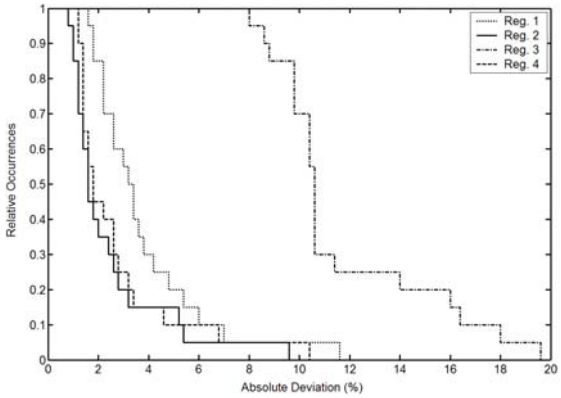

Fig. 4. SOE curves for different regression functions (L=L*).

4.2. Sliding Occurrence Error curves

In some industrial applications, the choice of a specific regression function only based on REC curves proves to be not adequate, since these curves give only integral information and do not provide any information about the time distance between regression errors.

On the other hand, this knowledge that provides a kind of "local accuracy" could provide some additional information useful to choose the more appropriate regression function. Indeed, in many contexts, once a suitable threshold has been fixed as the maximum tolerable error, it is preferable to use a regression function able to grant a small percentage of errors exceeding the threshold in a time interval (defined in the design phase) rather than a regression function that assures the lowest mean error (corresponding to the minimum AOC of the REC curves) even if characterized by some time windows in which a higher percentage of threshold overcoming occurs.

This is the case of the mass air flow sensor fault accommodation. In fact, the relatively slow engine and vehicle time dynamics allow also the use of prediction samples with even very high regression errors but characterized by a small number of occurrences in a suitable time interval. In this way, the correct management of the engine could still be assured in real-time.

Then, it is very helpful to build up suitable curves highlighting these aspects. To this aim let us to consider a window constituted by L samples (corresponding to a time interval $T = L \cdot T_S$, being T_S the sampling period). The *Sliding Occurrence Error* (*SOE*) curves plot the *error* tolerance (defined as the absolute deviation $|y - M_a|$) on the x-axis and the corresponding *relative occurrence* in L of the regression function on the y-axis. The intersection of the SOE curves with the x-axis provides the maximum percentage error made by the corresponding regression function in all L-length segments. As an example, Fig.4 shows the Sliding Occurrence Error curves for different regression functions, having fixed a window length $L = L^*$.

Of course the regression function corresponding to the curves closest to the y-axis (Reg. 2 and Reg. 4 in this case) offer the best performance while the worst case is achieved for Reg. 3. Nevertheless, for a selected Absolute Deviation, *AD*, these curves provide the relative occurrence, *RO*, of errors exceeding *AD* over a window length L of consecutive samples. Then, as an example, if we consider a target application with $AD = 5\,\%$ and $RO \leq 0.1$, only the regression function Reg.4 meet this requirement whereas for the same *AD*, Reg. 1, Reg. 2 and Reg. 4 are all adequate if the constraint is $RO \leq 0.3$.

Thanking to this further analysis, it is possible to verify if a given regression function really satisfies the design specifications also in terms of "local accuracy".

4.3. Computational burden

A realistic index useful to estimate the computational burden required by the run-time execution of ANNs is the number of multiplications to be carried out, being them more and more burdensome than sums or other elementary operations.

For single hidden layer MLP architectures, the general matrix representation is reported in Fig. 5. Then the ANN output is given by (1).

$$output = f_2 (\underline{\underline{LW}} \cdot f_1 (\underline{\underline{IW}} \cdot \underline{p} + \underline{b}_1) + \underline{b}_2) \qquad (1)$$

As a consequence, the number of multiplications required to achieve the ANN output are about $m = S_1 \cdot R + S_2 \cdot S_1$.

Referring to the considered ANN architectures (see section 2), S_1 ranges from 5 to 25, R from 2 to 12 for ANN_1/ANN_3 and from 3 to 18 for ANN_2, whilst S_2 is, in any case, equal to 1. Therefore, the value of m only depends on the number of both hidden nodes (S_1) and inputs (R).

5. EXPERIMENTAL RESULTS

In this section some experimental results are showed and commented. The criteria defined in the previous section are adopted to compare the ANNs features. In particular, three kinds of analysis are reported:

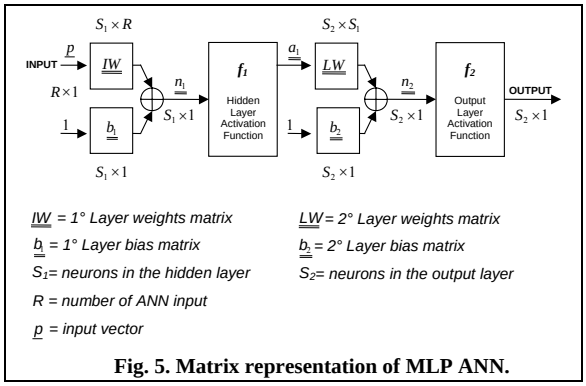

Fig. 5. Matrix representation of MLP ANN.

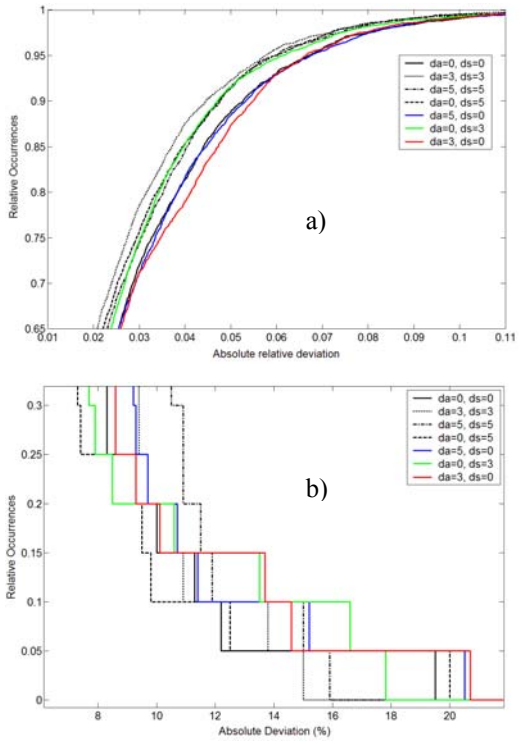

Fig. 6. a) REC curves and b) SOE curves (L = 20) for different ANN_1 input arrangements.

i) ANN tuning: considering (for the sake of brevity) one of the proposed ANN architecture, a performance comparison is carried out by varying the number of both inputs and hidden nodes;

ii) ANNs comparison: the performance comparison is carried out among ANN_1, ANN_2 and ANN_3 characterized by the best input arrangement and number of hidden nodes (evaluated in *i)*);

iii) Examples of ANN outputs: the ANN outputs (M_a) are plotted together with the actual values and the corresponding residuals.

5.1. ANN tuning

As an example, results for ANN_1 are reported with reference to the common rail system. The tuning was carried out by varying the number of hidden nodes and by considering different combination of number of inputs.

As for the hidden nodes, a number of 20 brought to noticeably best results in terms of accuracy with respect to 5, 10 and 15, whilst 25 nodes brought to not significant improvements. Therefore, the following results will be referred to a number of hidden nodes equal to 20.

As for the number of inputs, for sake of readability a reduced number of possible couple d_a-d_s will be considered. Fig. 6 shows the REC and SOE curves for the tested regression functions, having fixed $L = 20$, as assumable in this application in which the time dynamics are of some second's order and $T_S = 500$ ms ($T = L \cdot T_S = 10$ s). From the analysis of Fig. 6a, ANN_1 shows the best performance for d_a=3 and d_s=3 as confirmed by the AOC values, also if comparable behaviours are achievable with the couples d_a=5-d_s=5 and d_a=0-d_s=5. On the other hand, referring to Fig. 6b, if is required AD = 15 % with $RO \leq 0.05$, the goal is achievable only with d_a=3-d_s=3.

Table 1. Number of Multiplications (m) for different ANN_1 input arrangements and 20 hidden nodes.

d_a	0	3	5	0	5	0	3
d_s	0	3	5	5	0	3	0
m	60	180	260	160	160	120	120

Table 2. Best ANNs input arrangements for both engine systems.

Engine system	ANN_1	ANN_2	ANN_3
Common rail	d_a=3, d_s=3, 20 hidden nodes m=180	d_a=1, d_p=1, d_s=1, 20 hidden nodes m=140	d_a=5, d_p=5, 20 hidden nodes m=260
Injection pump	d_a=0, d_s=5, 20 hidden nodes m=160	d_a=1, d_p=1, d_s=1, 20 hidden nodes m=140	d_a=5, d_p=5, 20 hidden nodes m=260

As matter of fact, this target is very attractive for the considered application since the mass air flow sensor is often affected by gain faults (due to the aging and wear) greater than 20 % that however assures a still acceptable way engine management. Then, d_a=3-d_s=3 is selected for the best performance in terms of both mean and local accuracies. This choice is also adequate with respect to the computational burden as showed in Table 1 that reports the number of multiplications required for each couple d_a-d_s.

With the same analysis the best input arrangements and the number of hidden nodes were identified for ANN_2 and ANN_3. Table 2 summarizes these results for both engine systems highlighting also the number of multiplication required.

5.2. ANNs comparison

Starting form the results obtained in the tuning phase, a comparison among ANN_1, ANN_2 and ANN_3 can be carried out. Fig. 7 shows the REC and the SOE curves for the common rail system. The best performance with reference to both tools are achieved by ANN_2, that is also characterized by the lowest computational burden (see Table 2).

Similar investigations carried out on the injection pump system give the same results: ANN_2 with 20 hidden nodes and d_a=1, d_p=1, d_s=1 is characterized by the best features in terms of accuracies and computational burden.

5.3. Examples of ANN outputs

Fig.8 reports some examples of ANN output referred to both engine systems. The accommodated value M_a is obtained by considering the best architecture for ANN_2 (d_a=1, d_p=1, d_s=1). The results prove the very good agreement with actual values, also confirmed by residuals (absolute relative deviations) always less than 0.12. Good performance were obtained also by ANN_1 with residuals always less than 0.15 whilst, the worse behaviour was for ANN_3 (some residuals close to 0.30) as expected by the previous analyses (Fig.7).

6. CONCLUSIONS

The mass air flow sensor is a fundamental part of common rail and injection pump systems used in modern automotive turbocharged engines,. An artificial neural network based solution has been proposed in the paper, to allow the mass air flow meter fault accommodation. Several

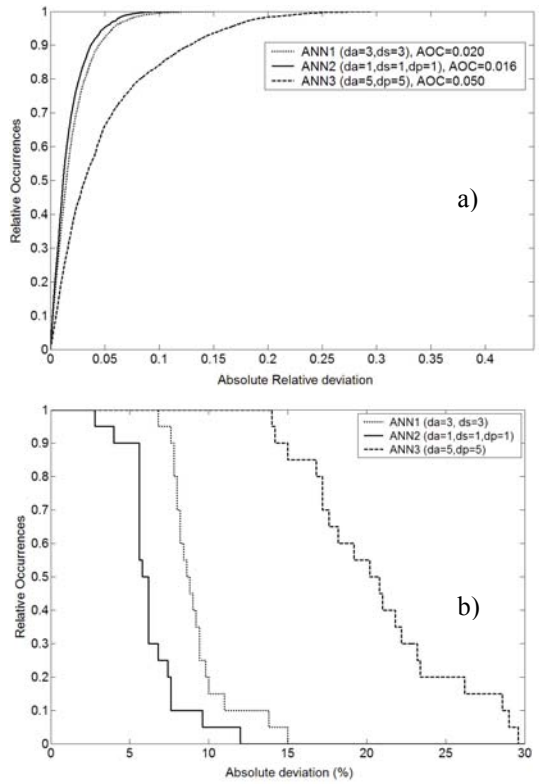

Fig. 7. Comparison of ANN_1, ANN_2 and ANN_3 for the common rail system: a) REC curves, b) SOE curves (L = 20).

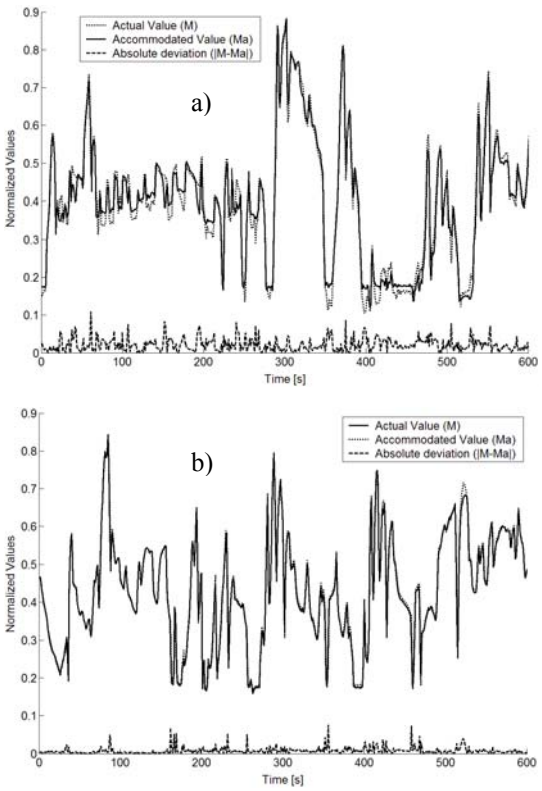

Fig. 8. Comparison between M and M_a for ANN_2 a) common rail system; b) injection pump system.

ANN architectures characterized by different input combinations (in number and type) as well as different number of hidden nodes and activation function were investigated. Their performance were compared by means of powerful graphical tools and computational load indexes. a The solution offering the best trade-off between accuracy and computational burden (ANN_2 with d_A=1, d_S=1, d_P=1) grants, in accommodation, regression errors never higher than 15 %, *mean error* close to 2 %, and *Relative Occurrences* (*RO*) ≤ 0.05 (having fixed L = 20 and an *Absolute Deviation* (*AD*) = 10 %). In addition, in any case, the computational burden required is compatible with on-board specifications [11]. Further improvements will concern with the integration of the proposed fault accommodation schemes in the ECU control software.

ACKNOWLEDGMENTS

The author wishes to thank the Dr. Antonio Cofano and the Autoconsulting Team for the significant help given in the experimental work.

REFERENCES

[1] W. J. Fleming, "Overview of Automotive Sensors", IEEE Sensors Journal, Vol. 1, NO. 4, December 2001, pp. 296-308.

[2] O. Schatz, "Recent Trends in Automotive Sensors", Proceedings of IEEE Sensors, October 2004, pp. 236-239.

[3] P. Schihl, "*Control Strategies for Heavy-Duty Diesel Engine Emissions*", IEEE Instrumentation and Measurement Magazine, June 2001, pp. 11-15.

[4] Heywood J.B., "Internal Combustion Engine Fundamental", MC Graw Hill. (1988).

[5] Chen J., Patton R. J., Liu J. P., "Detecting incipient sensor faults in flight control systems", Proc. Third IEEE Conf. Control Applications. Glasgow, U.K., August 1994, pp. 871-876.

[6] Pau-Lo Hsu, Ken-Li Lin, Li-Cheng Schen, "Diagnosis of Multiple Sensor and Actuator Failures in Automotive Engines", IEEE Transaction on Vehicular Technology, Vol. 44, NO 4, November 1995, 779-789.

[7] Dorr R., Kratz F., Ragot J., Loisy F., Germain J. L., "Detection isolation and identification of sensor faults in nuclear power plants", IEEE Trans. Contr. Syst. Technol, vol. 5, no. 1., 1997, pp. 42-60.

[8] Betta G., Pietrosanto A., "Instrument fault detection and isolation: state of the art and new research trends", IEEE Transaction on Instrument and Measurement, vol. 49., February 2000, pp. 100–107.

[9] P. J. Buehler, M. A. Franchek, I. Makki, "Mass Air Flow Sensor Diagnostics for Adaptive Fueling Control of Internal Combustion Engines", Proceedings of the American Control Conference, Anchorage, AK, May 2002, pp. 2064-2069.

[10] Capriglione D., Liguori C., Pietrosanto A., Pianese C., "On-line sensor fault detection, isolation and accommodation in automotive engines", Instrumentation and Measurement, IEEE Transaction on, Vol. 52, Issue 4, August 2003, pp. 1182-1189.

[11] Capriglione D., Liguori C., A. Pietrosanto.,"Real-time implementation of IFDIA scheme in automotive system", Proceedings of the 21-th IEEE Instrumentation and Measurement Technology Conference, Como, ITALY, Vol. 3., May 2004, pp. 1667-1672.

[12] Bernieri A., Betta G., Capriglione D., Molinara M., "SVM-Based Approach for Instrument Fault Accommodation in Automotive Systems", Proc. of IEEE Intern. Conf. on Virtual Environments, Human-Computer Interfaces and Measurement Systems, Giardini Naxos, ITALY, July 2005, pp. 145-150.

[13] J. Bi, K. P. Berrett - "Regression Error Characteristic Curves", Proceedings of the Twentieth International Conference on Machine Learning (ICML-2003), Washington DC, 2003.